



A modular platform for surface-bound biosensing: SpyCatcher-Mediated functionalization of antifouling polypeptide brushes on gold and polystyrene

Chuanbao Zheng^{a,b}, Zohaib Hussain^a, Amanda de Souza^{a,c}, Chang Chen^a,
Walter van Slooten^a, Siddharth Deshpande^a, Zhisen Zhang^d, Han Zuilhof^{b,e},
Renko de Vries^{a,*}

^a Physical Chemistry and Soft Matter, Wageningen University & Research, Stippeneng 4, 6708 WE, Wageningen, the Netherlands

^b Laboratory of Organic Chemistry, Wageningen University & Research, Stippeneng 4, 6708 WE, Wageningen, the Netherlands

^c Department of Biosciences, Federal University of São Paulo, 11015020, Santos, SP, Brazil

^d Research Institute for Biomimetics and Soft Matter, Fujian Provincial Key Laboratory for Soft Functional Materials Research, Department of Physics, Xiamen University, 361005, Xiamen, China

^e College of Biological, Chemical Science and Engineering, Jiaxing University, 314001, Jiaxing, China

ARTICLE INFO

Keywords:

Antifouling coating
SpyCatcher/SpyTag
QCM-D
Biosensors
Surface functionalization

ABSTRACT

Precise molecular engineering of surfaces is critical for advancing biosensing, antifouling technologies, and smart material interfaces, yet current methods often suffer from uncontrolled orientation or require complex surface chemical modifications. Here, we report a modular protein-based platform that combines two key elements: (1) self-assembling **B-M-E** protein antifouling brushes composed of a solid-binding peptide (**B**), a multimerization domain (**M**), and an antifouling polypeptide (**E**). (2) Bioorthogonal SpyCatcher/SpyTag chemistry for precise post-assembly covalent immobilization of target molecules with site-specific control. We demonstrate high-efficiency conjugation on both gold and polystyrene surfaces using quartz crystal microbalance with dissipation (QCM-D) and fluorescence assays. This bioorthogonal strategy offers one-step surface coating without complex chemical modifications, tunable and stable protein immobilization, and universal substrate compatibility. Our post-assembly functionalization platform provides a versatile toolbox for creating functional protein coatings by suppressing non-specific binding, which minimizes background interference and improves detection sensitivity and specificity. This approach holds significant potential for applications such as point-of-care diagnostics and continuous monitoring devices.

1. Introduction

Precise control over molecular composition and spatial organization of functional groups on solid surfaces is of fundamental importance in material science, biotechnology, and medicine (Jiang et al., 2020; Flynn et al., 2023; Song et al., 2024). From highly sensitive biosensors to long-lasting antifouling coatings, interfacial performance hinges on the ability to anchor bioactive molecules in a well-controlled manner under physiologically relevant conditions. Numerous coating strategies, including but not limited to oligo/poly(ethylene glycol) coatings (Ma et al., 2004; Hucknall et al., 2009; Heggstad et al., 2020; Riedel et al., 2013; Lowe et al., 2015; Banerjee et al., 2011), polylysine-mediated

coatings (Lebaudy et al., 2023; Tian et al., 2020), zwitterionic coatings (Cheng et al., 2009; Li et al., 2019) and peptides based coatings (Chelmowski et al., 2008; Chen et al., 2009; Nowinski et al., 2012; Alvisi et al., 2022), have been developed to meet the need of diverse antifouling applications. These developed coatings provide straightforward conjugation procedures and exhibit good to excellent antifouling properties on a wide range of surfaces. They further allow post-fabrication functionalization through the incorporation of a minor fraction of bio-reactive units (Postma et al., 2025).

Nevertheless, despite these advantages, conventional modification strategies are inherently limited by their chemical and structural simplicity, often lack the biomolecular complexity required to

* Corresponding author.

E-mail address: renko.devries@wur.nl (R. de Vries).

<https://doi.org/10.1016/j.bios.2025.118251>

Received 25 September 2025; Received in revised form 10 November 2025; Accepted 19 November 2025

Available online 21 November 2025

0956-5663/© 2025 The Authors. Published by Elsevier B.V. This is an open access article under the CC BY license (<http://creativecommons.org/licenses/by/4.0/>).

dynamically interface with biological systems. In contrast, protein-based coatings offer a powerful platform to mimic complex biological interfaces. A key advantage of such coating lies in genetic programmability, which allows for the precise integration of multiple functional domains within a single, seamlessly linked polypeptide chain.

In this way, genetically engineered polypeptides offer a modular and programmable alternative to traditional surface modification methods (Merkx et al., 2019; Chen et al., 2021; Alvisi and de Vries, 2023; Han et al., 2025). By leveraging the specificity of solid-binding peptide domains and the orthogonality of bioorthogonal chemistry (Alvisi and de Vries, 2023; Fu et al., 2024), polypeptides-based coatings enable precise control over interfacial properties. Our group recently developed a tri-block polypeptide architecture, termed **B-M-E** (Fig. 1c), which provides a robust and modular platform for creating tailor-made self-assembled antifouling polypeptide brush on diverse materials (oxides, metals, and plastics) (Alvisi et al., 2022; Zheng et al., 2023, 2025a, 2025b). In these modular designs, solid-binding peptides **B** are used to attach protein to solid surfaces (Brown, 1997; Hassert et al., 2012; Care et al., 2015). A de novo designed multimerization block **M** is used to enhance the coating stability and density through multivalency (Fallas et al., 2017). Finally, a hydrophilic, intrinsically disordered polypeptide block **E** is employed to provide antifouling functionality (MacEwan and Chilkoti, 2010; Varanko et al., 2020; Garanger and Lecommandoux, 2022; Guo et al., 2023; Strader et al., 2024). This fully recombinant system enables the creation of highly nonfouling interfaces without relying on synthetic polymers.

Despite the versatility of **B-M-E** coatings, strategies for bio-functionalization on surfaces remain limited. Over the past decades, strategies for cargo attachment via catalytic protein domains (Stagge et al., 2013; Sun et al., 2014, 2019; Buldun et al., 2018; Hatlem et al., 2019; Keeble et al., 2022; Krishnan et al., 2023) as well as site-specific chemical attachment to specific amino acid residues have been developed (Madl and Heilshorn, 2017; Zhang et al., 2016). In particular, the SpyTag (a 13-residue peptide) and its protein partner SpyCatcher, derived from the *Streptococcus pyogenes* fibronectin-binding protein, have gained significant attention due to their ability to spontaneously and irreversibly form a clean/mild isopeptide bond under physiological conditions (Zakeri et al., 2012; Keeble et al., 2017, 2019; Fu and Li, 2020; Kimura et al., 2021; Krishnan et al., 2024; Boonyakida et al., 2025). Such properties make it particularly well-suited for stable and site-specific conjugation in surface biofunctionalization for diverse applications.

In this study, we hypothesize that the incorporation of the SpyCatcher/SpyTag (Fig. 1a) system into the **B-M-E** polypeptide brushes (Fig. 1c) would enable covalent, site-specific, and modular post-assembly functionalization on different surfaces (Fig. 1d). To test this hypothesis, we employed the SpyCatcher003/SpyTag003 (Keeble et al., 2019) system (unless specified, referred to as SpyCatcher/SpyTag hereafter for simplicity), which exhibit higher reaction rate than earlier versions (Keeble et al., 2017; Zakeri et al., 2012). As a proof of concept,

we genetically fused super-folded green fluorescent protein (GFP) (Pédélecq et al., 2006) either to SpyCatcher or SpyTag as our model cargo protein to validate the platform (Fig. 1b). Protein purity was confirmed by sodium dodecyl sulfate-polyacrylamide gel electrophoresis (SDS-PAGE). Protein structural characterization by size-exclusion chromatography (SEC) and circular dichroism (CD) confirmed the proper folding and trimeric assembly of our functionalized polypeptides. We employed quartz crystal microbalance with dissipation (QCM-D) to quantitatively validate specific conjugation on both gold and polystyrene surfaces, complemented by macroscale visualization of the conjugation process in microfluidic channels. Building on this, this strategy moves beyond the passive antifouling **B-M-E** coating to establish a modular, genetically encoded platform for active and programmable biofunctionalization. By leveraging SpyCatcher/SpyTag chemistry, it paves the way for next-generation passive antifouling coatings, high-performance biosensors, and advanced therapeutic interfaces.

2. Results and discussion

2.1. Design and conceptual framework of **B-M-E**-SpyCatcher polypeptide brushes

Previously, we demonstrated that **B-M-E** coating proteins are modular and can be readily adapted to different surfaces by substituting the solid-binding **B** domain (Alvisi et al., 2022; Zheng et al., 2023, 2025a). In this study, we use sequences of previously designed unfunctionalized **B-M-E** proteins that self-assemble into antifouling brushes on gold (Zheng et al., 2023) and polystyrene (Zheng et al., 2025a) surfaces. As is shown in Fig. 1d, we genetically attach SpyCatcher domains to create the new tetrablocks **B^{Au}-M-E**-SpyCatcher with gold-binding peptides (one-letter amino acid code: MHGKTQATSGTIQS) (Brown, 1997) as surface anchors and **B^{PS}-M-E**-SpyCatcher with polystyrene-binding peptides (one-letter amino acid code: VHWDFRQWWQPS) (Qiang et al., 2017) as surface anchors. In contrast to simple physical adsorption, solid-binding peptides engage in multiple cooperative interactions that render them highly resistant to desorption (Tang et al., 2013; Zheng et al., 2025a). Next, we employed GFP either fused with SpyTag or SpyCatcher as a model system to test SpyCatcher/Tag conjugation (Pédélecq et al., 2006). We choose to attach the bulkier SpyCatcher to the coating protein rather than the SpyTag, since we anticipate that typically users want to use cargo (to be attached to the coating) tagged with the small SpyTag peptide.

We hypothesized that the **B-M-E**-SpyCatcher tetrablock retains its ability to prevent nonspecific protein adsorption through the antifouling **E** domain, while the terminal SpyCatcher domain enables site-specific covalent conjugation with SpyTag-fused cargo proteins. Detailed sequences of primers, DNA and amino acids sequences used in this study are provided in Tables S1–S3. All expression plasmids were sequence-

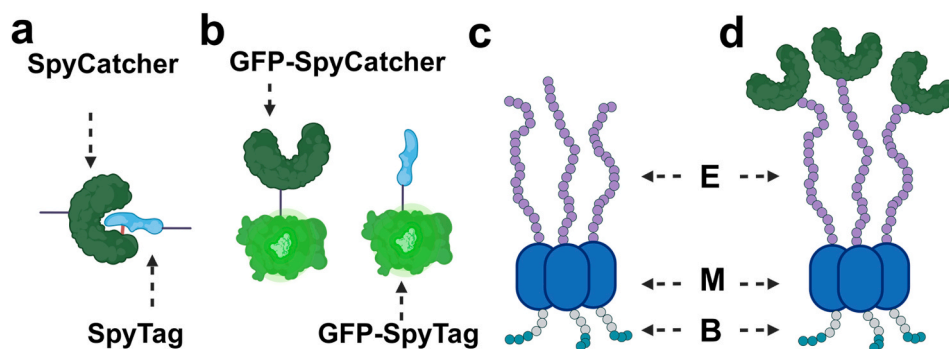


Fig. 1. Schematic representation of constructs used in this study. a) SpyCatcher/Tag system. b) GFP-SpyCatcher and GFP-SpyTag fusions. c) **B-M-E** triblock coating proteins binding to either gold- or polystyrene surfaces. d) Fusions of SpyCatcher with gold- and polystyrene-coating **B-M-E** proteins.

verified prior to being transformed into *E. coli*. Proteins were purified using immobilized metal affinity chromatography (IMAC), followed by size exclusion chromatography (SEC). Protein integrity and purity were confirmed by SDS-PAGE. Molecular weights of the purified proteins are determined using MALDI-TOF (Fig. S1 and Table S4). Materials and Methods are provided in Support Information.

2.2. Trimer formation and SpyCatcher functional group presentation in solution

Next, we investigated the secondary structure of engineered proteins, with particular attention to the proper folding of the **M** domain in the context of the tetrablocks, by SEC and CD spectroscopy (Fig. 2). As shown in Fig. 2a, the SEC retention volumes for the gold- and polystyrene-binding **B-M-E**-SpyCatcher proteins were approximately 10-11 mL. This aligns well with our previous studies, where the unfunctionalized **B-M-E** exhibited similar retention volumes (~11 mL) (Zheng et al., 2023, 2025a). The observed similar retention volumes suggest that the SpyCatcher domain did not significantly alter the hydrodynamic volume of the complex, which is consistent with its relatively small size with a hydrodynamic diameter of 3.6 nm (Tyler et al., 2023). Previously, we have demonstrated that the **B-M-E** proteins (depending on the size of the **E** block) form a monomolecular coating with a layer thickness of 13-20 nm (Zheng et al., 2023, 2025a). This coating thickness is within the effective penetration depth of the surface plasmon resonance evanescent field (typically 100-300 nm) (Abbas et al., 2011; Bajaj et al., 2023). Additionally, the retention volumes found are smaller than that of previously reported (Zheng et al., 2025b) bovine serum albumin (BSA, ~66 kDa, ~14 mL). Given that the molecular weight of **B-M-E**-SpyCatcher monomer (~56 kDa) is smaller than that of BSA, the observed SEC profiles strongly suggest that **B-M-E**-SpyCatcher proteins oligomerize in solution, consistent with the formation of the designed trimeric complex (~168 kDa, ~10 mL), as we have previously reported (Zheng et al., 2023, 2025a, 2025b).

To complement the SEC data, CD spectroscopy was employed to confirm the protein secondary structure. The CD signal is expected to be dominated by the α -helical **M** domain, as the unstructured **B** and **E** domains contribute minimally, and the β -sheet-rich SpyCatcher domain is relatively small compared to the **M** block. Indeed, as shown in Fig. 2b, the CD spectra of the **B-M-E**-SpyCatcher proteins are consistent with those previously reported for unfunctionalized **B-M-E** proteins (Alvisi et al., 2022; Zheng et al., 2023, 2025a, 2025b), displaying features characteristic of high α -helical content (with characteristic double minima around 208 nm and 222 nm). In contrast, CD spectra for the GFP fusion proteins have more characteristic of β -sheet rich proteins (with a characteristic of single minimum around 219 nm), as expected.

Subsequently, we evaluated the functionality of the SpyCatcher/

SpyTag proteins in solutions by examining covalent bond formation using SDS-PAGE (Fig. 3). Protein samples were mixed in PBS for 5 min prior to analysis. In Fig. 3a, lane 2 corresponds to purified **B^{Au}-M-E**-SpyCatcher. Lanes 3 and 4 correspond to **B^{Au}-M-E**-SpyCatcher mixed with GFP-SpyCatcher and GFP-SpyTag, respectively. The higher-molecular-weight conjugates observed in lane 4 confirms covalent reaction between **B^{Au}-M-E**-SpyCatcher and GFP-SpyTag. As anticipated, no reaction occurs between **B^{Au}-M-E**-SpyCatcher and GFP-SpyCatcher (Fig. 3a, lane 3). Similar results are found for **B^{PS}-M-E**-SpyCatcher when mixed with GFP-SpyTag and additional (non-reactive) **B^{PS}-M-E** (Fig. 3b). We do observe that a small fraction of **B^{PS}-M-E**-SpyCatcher remains unreacted after 5 min incubation with GFP-SpyTag (Fig. 3b, lane 6). Nevertheless, taken together, the results confirm that the SpyCatcher unit remains functional when genetically fused to the **B-M-E** proteins. Additional SDS-PAGE analyses for the reaction between **B^{Au}-M-E** and GFP-SpyCatcher/Tag, as well as between GFP-SpyCatcher and GFP-SpyTag, are shown in Fig. S2a and S2b, respectively.

2.3. Surface assembly and site-specific functionalization via SpyCatcher/SpyTag

To evaluate immobilization of proteins and site-specific functionalization of the surfaces, we conducted QCM-D experiments on both gold and polystyrene surfaces (see Fig. 4). QCM-D enables real-time, label-free monitoring of both mass adsorption and the viscoelastic properties of surface-bound layers. These properties make it an ideal tool for assessing not only the immobilization of proteins, but also of the structural stability and rigidity of the resulting surface coating. To mitigate potential steric hindrance of the SpyCatcher domains when presented at a high surface density, we coated the surfaces with a 1:1 mixture of **B-M-E** and **B-M-E**-SpyCatcher. Following coating of the sensor surfaces, GFP-SpyCatcher or GFP-SpyTag were injected into the QCM-D flow channels to test reactivity and potential non-specific binding. First, we tested the gold-binding variants of the proteins, performing QCM-D with gold-coated quartz sensors. As shown in Fig. 4a, injection of Au-coating protein (1:1 mixture of **B^{Au}-M-E** and **B^{Au}-M-E**-SpyCatcher) led to a marked frequency decrease, indicating rapid and efficient surface coating. The flat QCM-D signal during the PBS rinse demonstrates the coating is stable for prolonged rinsing with PBS. Upon injection of GFP-SpyCatcher (green line with circles in Fig. 4a), negligible frequency shifts were observed, suggesting minimal nonspecific binding to the antifouling brush. This demonstrates that the antifouling function of the **E** domain is preserved also in the presence of the SpyCatcher domain. In contrast, injection of GFP-SpyTag (blue line with triangles in Fig. 4a) resulted in a significant frequency drop (see zoomed-in signal in Fig. 4c), consistent with rapid covalent conjugation and increased surface mass. During the subsequent PBS rinse, the frequency

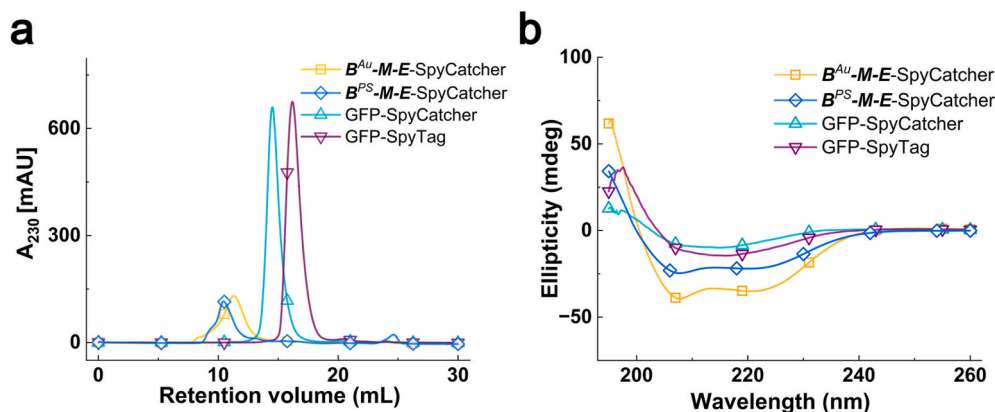


Fig. 2. Characterization of protein constructs. a) SEC analysis. Absorbance at 230 nm (A_{230}) as a function of retention volume. b) CD spectra displaying ellipticity (mdeg) versus wavelength (nm). CD measurements were performed at 0.1 mg/mL protein concentration in PBS, recorded at 20 °C.

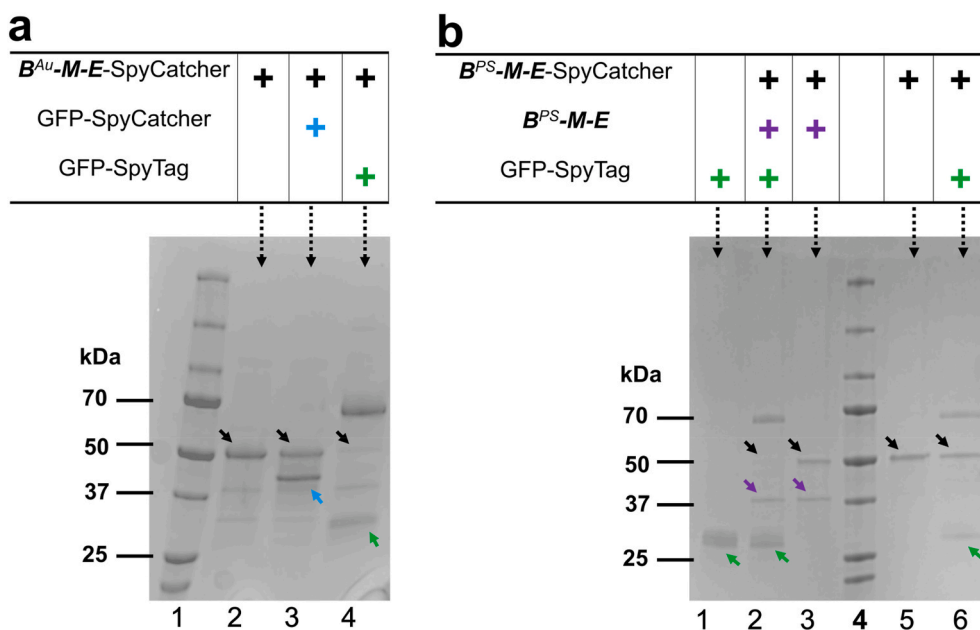


Fig. 3. SDS-PAGE analysis confirms protein purity and reactivity. a) Reactivity of gold-binding tetrablocks $B^{Au}-M-E$ -SpyCatcher with GFP-SpyCatcher and GFP-SpyTag. b) Reactivity of triblock $B^{PS}-M-E$ and tetrablock $B^{PS}-M-E$ -SpyCatcher with GFP-SpyTag. Molecular mass markers are presented in lane 1 for a) and lane 4 for b), respectively. Protein bands are indicated by small arrows in matching colors.

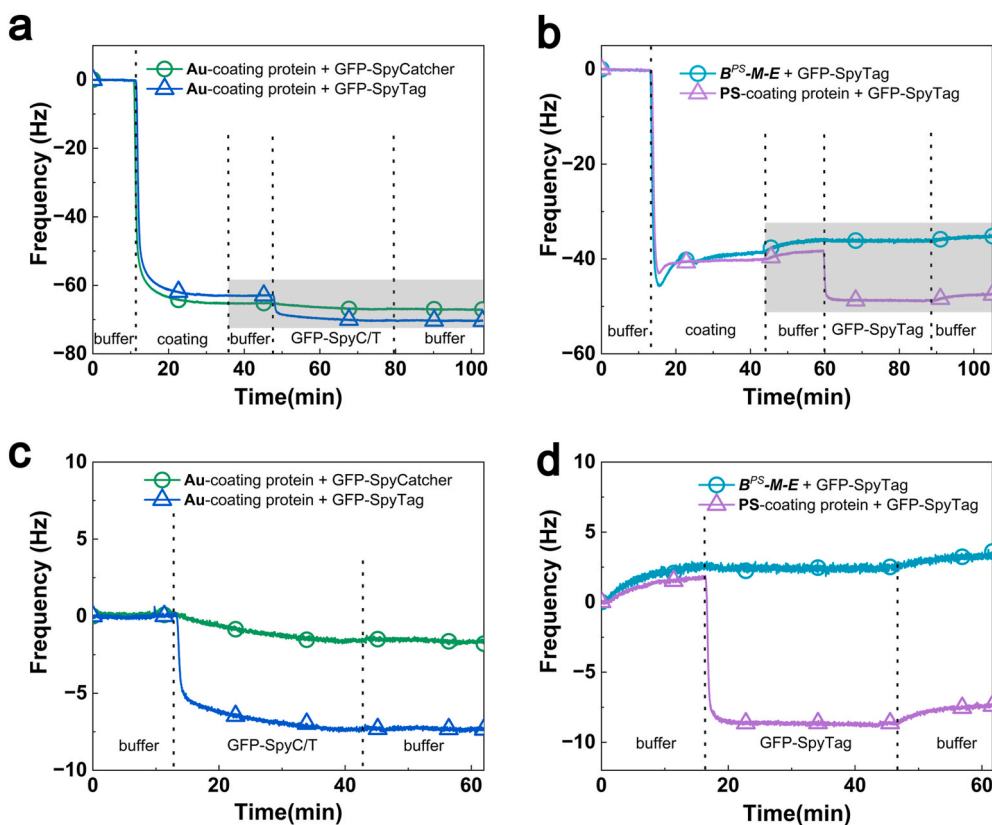


Fig. 4. Real-time surface assembly and functionalization of $B-M-E$ brushes monitored by QCM-D. a) Specific sensing of GFP-SpyCatcher (green line with circles) and GFP-SpyTag (blue line with triangles) on gold surfaces. Au-coating protein refers to $B^{Au}-M-E + B^{Au}-M-E$ -SpyCatcher in a 1:1 M ratio ($5 \mu\text{M}:5 \mu\text{M}$) applied to gold surfaces. b) Specific sensing of GFP-SpyTag on polystyrene surfaces. PS-coating protein refers to $B^{PS}-M-E + B^{PS}-M-E$ -SpyCatcher with 1:1 M ratio ($2.8 \mu\text{M}:2.8 \mu\text{M}$) applied to polystyrene surfaces (purple line with triangles). Polystyrene surfaces coated only with $B^{PS}-M-E$ (cyan line with circles). c) Enlarged view of the gray highlighted region in Fig. 4a with the baseline frequency of the coated sensor set to 0 Hz. d) Enlarged view of gray highlighted region in Fig. 4b with the baseline frequency of the coated sensor set to 0 Hz. PBS is indicated as buffer. GFP-SpyC/T refers to GFP-SpyCatcher and GFP-SpyTag, respectively.

remained stable, confirming the specificity and irreversibility of the SpyCatcher/SpyTag bond formation. The corresponding dissipation data (Fig. S3a) further support the formation of a stable protein layer.

Encouraged by the results on gold surfaces, we next tested whether our design could be extended to non-metallic surfaces. QCM-D sensors coated with polystyrene were used as a model for plastic substrates because polystyrene is a common material for microfluidic devices and well plates—to its direct applicability in lab-on-a-chip and continuous sensing systems. This study employed a step-by-step experimental strategy to validate the platform. The specific, covalent nature of the conjugation was first established on gold by contrasting the strong positive signal from GFP-SpyTag with the null response from the structurally matched negative control, GFP-SpyCatcher (Fig. 4a).

With this orthogonality confirmed, subsequent experiments on polystyrene focused on quantifying the conjugation efficiency of the positive reaction (GFP-SpyTag), leveraging the already-demonstrated specificity of the SpyCatcher/SpyTag system. Therefore, only GFP-SpyTag was selected for testing the orthogonality on polystyrene surfaces. Two types of channels were prepared: one coated with $B^{PS}\text{-M-E}$ alone, the other coated with PS-coating protein (1:1 M ratio mixture of $B^{PS}\text{-M-E}$ and $B^{PS}\text{-M-E-SpyCatcher}$). As shown in Fig. 4b, during the protein coating phase, the frequency signal did not decrease monotonically as it did for the gold-binding proteins on the gold surfaces. Instead, there was a small overshoot eventually followed by signal stabilization. This dynamic behavior may reflect a Vroman-like effect (Hirsh et al., 2013) or transient aggregation followed by reorganization of the coating proteins on the hydrophobic polystyrene surface. Note that the polystyrene-binding peptides of the coating proteins (one-letter amino acid code: VHWDFRQWWQPS)(Qiang et al., 2017) contain three tryptophan (W) residues and one phenylalanine (F) residue, which could lead to some degree of self-assembly of the coating proteins in solution, which would require conformational rearrangements upon adsorption on surfaces. Similar behavior was reported in our earlier study on the coating of polystyrene surfaces with $B^{PS}\text{-M-E}$ triblock proteins (Zheng et al., 2025a). Following PBS rinsing, a slight upward shift in frequency was observed in both channels, indicating the removal of some loosely adsorbed protein. After this transient signal, we found good stability of the surface-bound layer for prolonged rinsing with PBS. Upon injection of GFP-SpyTag, the surface coated with $B^{PS}\text{-M-E}$ alone showed no detectable frequency shift, confirming minimal nonspecific adsorption. In contrast, the surface coated with 1:1 $B^{PS}\text{-M-E} + B^{PS}\text{-M-E-SpyCatcher}$ exhibited a substantial frequency decrease, indicating successful and specific covalent conjugation between surface-bound SpyCatcher and GFP-SpyTag. The final PBS rinsing step confirms the irreversible nature of the interaction. Dissipation data for these QCM-D experiments are given in Figure S3a and Figure S3b.

Our earlier studies showed that gold-coating proteins at a concentration of 10 μM and polystyrene-coating proteins at a concentration of 5 μM form a saturated coating layer on the respective surfaces (Zheng et al., 2023, 2025a). Under this premise of saturated coverage, the larger initial frequency shift on gold (-60 Hz vs. -40 Hz on PS) indicates the formation of a thicker, more extended, and highly hydrated brush structure (Fig. 4a and b). Crucially, despite this higher degree of hydration and a likely higher initial areal density of SpyCatcher proteins, the subsequent cargo conjugation was less efficient on gold ($\Delta F = -7.3$ Hz) than on polystyrene ($\Delta F = -10.4$ Hz). We attribute this difference to steric accessibility: the dense, thick brush on gold sterically masks a significant fraction of its SpyCatcher domains, rendering them inactive. This is proved by the minimal dissipation change during conjugation on gold ($\Delta D = +0.32$ ppm). This indicated that the reaction occurs with little perturbation to the pre-formed brush on gold surfaces. In contrast, coating on polystyrene presents its SpyCatcher moieties with higher accessibility, leading to a higher conjugation efficiency. This is supported by the larger frequency shift and substantial dissipation increase on polystyrene ($\Delta D = +0.63$ ppm) further suggests that the conjugation process may involve a beneficial reorganization of the interface to

maximize cargo loading. While precise absolute density determination can be obtained using Sauerbrey equation (Sauerbrey, 1959; Yang et al., 2025) if the coating layer is rigid. However, our system's hydrated flexible E block may not fully meet this criterion. Thus, while the absolute densities are first-order approximations, the calculated $\sim 40\%$ loading density is higher on polystyrene versus gold (Supplementary Information, Note S1). Together, these data confirm: the structural integrity and antifouling performance of the $B\text{-M-E}$ coatings during functionalization, and the formation of specific, covalent SpyCatcher/SpyTag complexes rather than nonspecific adsorption. Also, this establishes an important design principle: the optimal coating architecture for functionalization is not necessarily the one that binds the most protein, but the one that presents the most functional groups in an accessible manner.

The performance of the coating, including its stability and ability to resist nonspecific adsorption in complex media, is critical for its practical application. Here, we define stability as the structural integrity of the coating within a typical assay timeframe. We next evaluated its performance on polystyrene substrates. The results show that the $B^{PS}\text{-M-E} + B^{PS}\text{-M-E-SpyCatcher}$ brush after GFP-SpyTag functionalization is highly stable over 30 min in 10 % human serum (HS, Fig. 5a). Furthermore, the coating effectively retained its antifouling property under these conditions, indicating that the conjugation chemistry and brush architecture remain intact in biologically relevant environments. In Fig. 5b, the fouling percentage of the $B^{PS}\text{-M-E} + B^{PS}\text{-M-E-SpyCatcher}$ functionalized surface ($\sim 9.5\%$) was drastically lower than that of bare polystyrene as reported earlier (Zheng et al., 2025a). The fouling percentage calculation method was described elsewhere (Zheng et al., 2025b). The dash line with an arrow is the fouling percentage of surface coated with $B^{PS}\text{-M-E}$ ($\sim 6\%$). Additional dissipation data further support the coating stability in diluted HS (Fig. S4). The complete QCM-D data on polystyrene surfaces are provided in Fig. S5.

2.4. Fluorescence visualization confirms functionalized surface reactivity

While QCM-D provides molecular-level insights into the real-time binding kinetics and surface mass adsorption, fluorescence imaging offers complementary, application-relevant validation by visually confirming successful surface functionalization. Therefore, we replicated the QCM-D functionalization conditions in polystyrene microfluidic channels. The surfaces of these channels were coated either with $B^{PS}\text{-M-E}$ alone or with a 1:1 mixture of $B^{PS}\text{-M-E} + B^{PS}\text{-M-E-SpyCatcher}$. Additionally, we included an uncoated channel as a reference. Next, these channels were exposed to GFP-SpyTag and imaged using fluorescence microscopy. As shown in Fig. 6a, the uncoated polystyrene channels exhibited strong nonspecific (possibly multilayer) adsorption of GFP-SpyTag, resulting in a strong fluorescence signal. In contrast, weaker and uniform fluorescence due to specific chemical conjugation was observed for channels coated with the $B^{PS}\text{-M-E} + B^{PS}\text{-M-E-SpyCatcher}$ mixture (Fig. 6b). The intensity was approximately one third of that of the uncoated surfaces, indicating a dense adsorption of the GFP-SpyTag construct onto uncoated PS channels. This suggests that a satisfyingly high fraction of the SpyCatcher moieties in the 1:1 mixture of protein is actually linked to the GFP-SpyTag. Finally, channels coated solely with $B^{PS}\text{-M-E}$ showed negligible fluorescence (Fig. 6c), as expected for a channel with a nonreactive coating with excellent antifouling properties (Zheng et al., 2025a). Quantitative analysis of normalized fluorescence intensity is provided in Fig. 6d. Together, these results support the QCM-D findings, demonstrate the robustness of this post-assembly conjugation strategy for stable, site-specific surface functionalization, and highlight its potential for biosensing and diagnostic applications.

The modular design of our platform also opens the possibility of performing the SpyCatcher/SpyTag conjugation step directly in complex media, such as cell lysates or crude protein extracts, rather than solely in purified buffer systems. Earlier report employed SpyTag-SpyCatcher

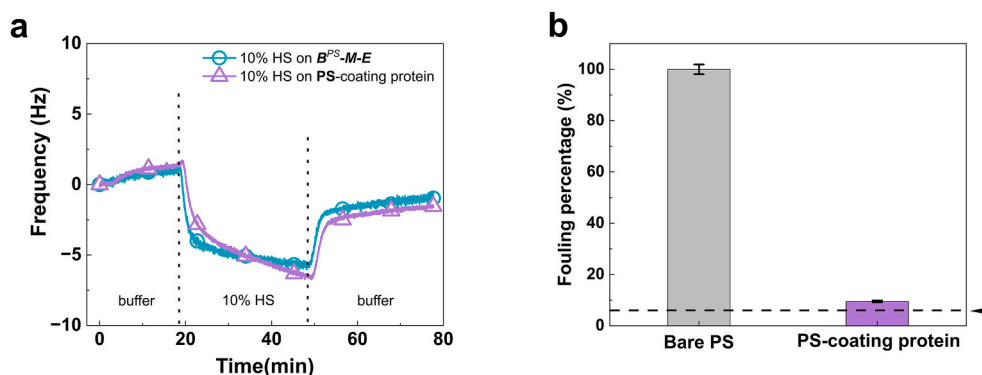


Fig. 5. QCM-D antifouling assay of adsorption of 10 % HS after GFP-SpyTag functionalization. a) QCM-D frequency data of 10 % HS adsorption on $B^{PS}\text{-M-E}$ (cyan line with circles) and $B^{PS}\text{-M-E} + B^{PS}\text{-M-E-SpyCatcher}$ (purple line with triangles) coated polystyrene surfaces. b) QCM-D dissipation data of 10 % HS adsorption. The dash line with an arrow indicates the fouling percentage of surface coated with $B^{PS}\text{-M-E}$.

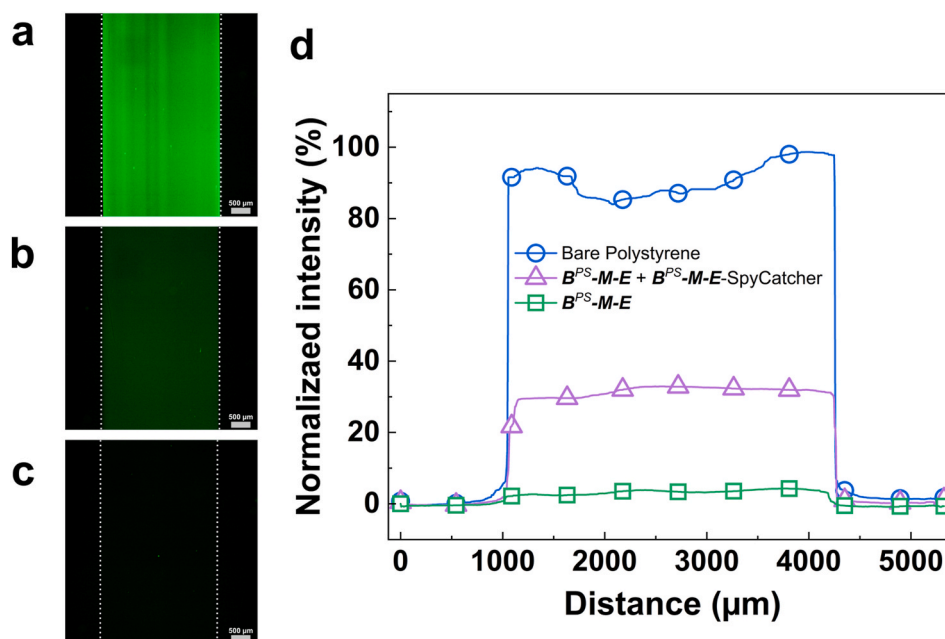


Fig. 6. Fluorescence microscopy of polystyrene microfluidic channels with various coatings, after the addition of GFP-SpyTag and PBS rinsing. a) Strong nonspecific adsorption of GFP-SpyTag on uncoated polystyrene surface (blue line with circles). b) Chemical conjugation of GFP-SpyTag to polystyrene channel coated with 1:1 $B^{PS}\text{-M-E} + B^{PS}\text{-M-E-SpyCatcher}$ (purple line with triangles). c) Minimal signal for GFP-SpyTag added to channel with $B^{PS}\text{-M-E}$ antifouling coating (green line with rectangles). d) Fluorescence intensity normalized to the value of the uncoated polystyrene channel. Scale bar in a), b) and c) is 500 μm .

reaction to purify SpyTag-linked protein from crude protein extract (Khairil Anuar et al., 2019). Therefore, the modularity of our platform presents a transformative model for diagnostic biosensing in complex solutions. It enables a ‘plug-and-play’ paradigm where a sensor chip, pre-coated with the $B\text{-M-E-SpyCatcher}$ brush, can be rapidly functionalized with any commercially available SpyTag-fused antibody or other biorecognition elements. This platform facilitates the creation of highly specific, antifouling sensing interfaces without the need for sample pre-treatment. This capability directly addresses the core principle of diagnostic testing by minimizing analyte manipulation and paves the way for versatile point-of-care devices.

3. Concluding remarks

We developed a modular and genetically encoded platform for site-specific and stable surface functionalization of generically antifouling brushes using SpyCatcher-functionalized $B\text{-M-E}$ polypeptide brushes. This biospecific platform enables post-assembly covalent

immobilization of cargo proteins on gold, polystyrene and other surfaces (for which solid-binding peptides are available) under mild, aqueous conditions. Using a combination of QCM-D analysis and fluorescence imaging in microfluidic channels, we demonstrated robust, irreversible binding across chemically distinct interfaces with minimal nonspecific adsorption. Importantly, the antifouling properties and modular architecture of the $B\text{-M-E}$ brushes, combined with the orthogonality and kinetic efficiency of the SpyCatcher/SpyTag reaction, make this system a versatile toolkit for surface biofunctionalization.

One of the distinct advantages of genetically encoded antifouling polypeptides is the ability to fuse functional peptides or proteins directly to the antifouling block (E), generating tetrablock constructs that directly self-assemble into functionalized brushes. While such a pre-assembly functionalization is straightforward and effective, it also presents limitations: each new functional domain requires new protein expression and purification, and surface adsorption of certain cargos may interfere with proper coating formation. These considerations highlight the value of the complementary post-functionalization

strategy we have developed here, enabling modular surface tailoring without compromising the antifouling base layer. Additionally, this approach represents a shift from passive antifouling toward active bio-functionalization, extending the functionality of the **B-M-E** coating. Importantly, the stability of the solid-binding peptides (**B**), combined with the covalent nature of the Spy chemistry, suggests that our platform is highly suitable for reusable devices and long-term storage. Future work will quantify the shelf-life of pre-functionalized surfaces and their performance over multiple regeneration cycles, which is a critical step towards commercial applications.

Building on this foundation, the platform also opens avenues for integrating responsive or stimuli-triggered elements, enabling dynamic control over surface functionalities. For example, coupling the Spy-Catcher/SpyTag system with other orthogonal conjugation pairs (e.g. SnoopCatcher/SnoopTag) or stimuli-responsive motifs (e.g., pH-, redox-, or ultrasound-responsive motifs) could allow reversible or conditional cargo presentation in real time (Buldun et al., 2018; de Haas et al., 2023; Lennicke and Cochemé, 2021; Hahmann et al., 2024). Furthermore, by incorporating cell-targeting ligands (e.g., RGD motif) or leveraging engineered protein or antibody (Ligorio and Mata, 2023; Dai et al., 2020), this approach would enable the creation of spatially organized and functionally diverse biointerfaces. Such surfaces could support next-generation applications in tissue engineering, point-of-care diagnostics, and implantable therapeutic devices (Kinnamon et al., 2022; Ligorio and Mata, 2023). Altogether, this genetically encodable and modular strategy provides a robust foundation for designing multifunctional, adaptive, and application-tailored protein-based biointerfaces.

CRediT authorship contribution statement

Chuanbao Zheng: Writing – review & editing, Writing – original draft, Methodology, Formal analysis, Data curation, Conceptualization. **Zohaib Hussain:** Writing – review & editing, Data curation. **Amanda de Souza:** Writing – review & editing, Data curation. **Chang Chen:** Writing – review & editing, Data curation. **Walter van Slooten:** Writing – review & editing, Data curation. **Siddharth Deshpande:** Writing – review & editing, Supervision. **Zhisen Zhang:** Writing – review & editing, Supervision. **Han Zuilhof:** Writing – review & editing, Supervision. **Renko de Vries:** Writing – review & editing, Writing – original draft, Supervision, Methodology, Conceptualization.

Notes

The authors declare no competing financial interest.

Declaration of competing interest

The authors declare that they have no known competing financial interests or personal relationships that could have appeared to influence the work reported in this paper.

Acknowledgments

C.Z acknowledges a fellowship from the China Scholarship Council (No. 202006310052). A.S. acknowledges a fellowship from APESP 2023/07102-5. S.D. and C.C. acknowledge financial support from Dutch Research Council (grant number: OCENW. KLEIN. 465).

Appendix A. Supplementary data

Supplementary data to this article can be found online at <https://doi.org/10.1016/j.bios.2025.118251>.

Data availability

We have shared all the necessary information in supporting information to reproduce our results.

References

- Abbas, A., Linman, M.J., Cheng, Q., 2011. New trends in instrumental design for surface plasmon resonance-based biosensors. *Biosens. Bioelectron.* 26, 1815–1824. <https://doi.org/10.1016/j.bios.2010.09.030>.
- Alvisi, N., de Vries, R., 2023. Biomedical applications of solid-binding peptides and proteins. *Mater. Today Bio* 19, 100580. <https://doi.org/10.1016/j.mtbio.2023.100580>.
- Alvisi, N., Zheng, C., Lokker, M., Boekestein, V., de Haas, R., Albada, B., de Vries, R., 2022. Design of polypeptides self-assembling into antifouling coatings: exploiting multivalency. *Biomacromolecules* 23, 3507–3516. <https://doi.org/10.1021/acs.biomac.2c00170>.
- Bajaj, A., Abutoama, M., Isaacs, S., Abuleil, M.J., Yaniv, K., Kushmaro, A., Modic, M., Cvelbar, U., Abdulhalim, I., 2023. Biofilm growth monitoring using guided wave ultralong-range surface plasmon resonance: a proof of concept. *Biosens. Bioelectron.* 228, 115204. <https://doi.org/10.1016/j.bios.2023.115204>.
- Banerjee, I., Pangule, R.C., Kane, R.S., 2011. Antifouling coatings: recent developments in the design of surfaces that prevent fouling by proteins, bacteria, and marine organisms. *Adv. Mater.* 23, 690–718. <https://doi.org/10.1002/adma.201001215>.
- Boonyakida, J., Matsuda, M., Suzuki, R., Muthuraman, K.R., Park, E.Y., 2025. Virus-like particle-based multiserotype quartet vaccine of dengue envelope protein domain III elicited potent anti-dengue responses. *Biomacromolecules* 26, 4449–4463. <https://doi.org/10.1021/acs.biomac.5c00459>.
- Brown, S., 1997. Metal-recognition by repeating polypeptides. *Nat. Biotechnol.* 15, 269–272. <https://doi.org/10.1038/nbt0397-269>.
- Buldun, C.M., Jean, J.X., Bedford, M.R., Howarth, M., 2018. SnoopLigase catalyzes peptide–peptide locking and enables solid-phase conjugate isolation. *J. Am. Chem. Soc.* 140, 3008–3018. <https://doi.org/10.1021/jacs.7b13237>.
- Care, A., Bergquist, P.L., Sunna, A., 2015. Solid-binding peptides: smart tools for nanobiotechnology. *Trends Biotechnol.* 33, 259–268. <https://doi.org/10.1016/j.tibtech.2015.02.005>.
- Chelmoski, R., Köster, S.D., Kerstan, A., Prekelt, A., Grunwald, C., Winkler, T., Metzler-Nolte, N., Terfort, A., Wöll, C., 2008. Peptide-based SAMs that resist the adsorption of proteins. *J. Am. Chem. Soc.* 130, 14952–14953. <https://doi.org/10.1021/ja8065754>.
- Chen, M., Fu, X., Chen, Z., Liu, J., Zhong, W.-H., 2021. Protein-engineered functional materials for bioelectronics. *Adv. Funct. Mater.* 31, 2006744. <https://doi.org/10.1002/adfm.202006744>.
- Chen, S., Cao, Z., Jiang, S., 2009. Ultra-low fouling peptide surfaces derived from natural amino acids. *Biomaterials* 30, 5892–5896. <https://doi.org/10.1016/j.biomaterials.2009.07.001>.
- Cheng, G., Li, G., Xue, H., Chen, S., Bryers, J.D., Jiang, S., 2009. Zwitterionic carboxybetaine polymer surfaces and their resistance to long-term biofilm formation. *Biomaterials* 30, 5234–5240. <https://doi.org/10.1016/j.biomaterials.2009.05.058>.
- Dai, Y., Xu, W., Liu, C.C., 2020. Immunoglobulin G-Based steric hindrance assay for protein detection. *ACS Sens.* 5, 140–146. <https://doi.org/10.1021/acssensors.9b01902>.
- de Haas, R.J., Ganar, K.A., Deshpande, S., de Vries, R., 2023. pH-Responsive elastin-like polypeptide designer condensates. *ACS Appl. Mater. Interfaces* 15, 45336–45344. <https://doi.org/10.1021/acsami.3c11314>.
- Fallas, J.A., Ueda, G., Sheffler, W., Nguyen, V., McNamara, D.E., Sankaran, B., Pereira, J. H., Parmeggiani, F., Brunette, T.J., Cascio, D., Yeates, T.R., Zwart, P., Baker, D., 2017. Computational design of self-assembling cyclic protein homo-oligomers. *Nat. Chem.* 9, 353–360. <https://doi.org/10.1038/nchem.2673>.
- Flynn, C.D., Chang, D., Mahmud, A., Yousefi, H., Das, J., Riordan, K.T., Sargent, E.H., Kelley, S.O., 2023. Biomolecular sensors for advanced physiological monitoring. *Nat. Rev. Bioeng.* 1, 560–575. <https://doi.org/10.1038/s44222-023-00067-z>.
- Fu, C., Wang, Z., Zhou, X., Hu, B., Li, C., Yang, P., 2024. Protein-based bioactive coatings: from nanoarchitectonics to applications. *Chem. Soc. Rev.* 53, 1514–1551. <https://doi.org/10.1039/D3CS00786C>.
- Fu, L., Li, H., 2020. Toward quantitative prediction of the mechanical properties of tandem modular elastomeric protein-based hydrogels. *Macromolecules* 53, 4704–4710. <https://doi.org/10.1021/acs.macromol.0c00664>.
- Garanger, E., Lecommandoux, S., 2022. Emerging opportunities in bioconjugates of Elastin-like polypeptides with synthetic or natural polymers. *Adv. Drug Deliv. Rev.* 191, 114589. <https://doi.org/10.1016/j.addr.2022.114589>.
- Guo, Y., Liu, S., Jing, D., Liu, N., Luo, X., 2023. The construction of elastin-like polypeptides and their applications in drug delivery system and tissue repair. *J. Nanobiotechnol.* 21, 418. <https://doi.org/10.1186/s12951-023-02184-8>.
- Hahmann, J., Ishaqat, A., Lammers, T., Herrmann, A., 2024. Sonogenetics for monitoring and modulating biomolecular function by ultrasound. *Angew. Chem. Int. Ed.* 63, e202317112. <https://doi.org/10.1002/anie.202317112>.
- Han, Y., Wu, Y., Lu, J., Liang, Q., Qu, X., Li, J., Miao, P., Yang, J., Li, G., 2025. Construction of bifunctional protein/peptide complex for sensitive detection of transglutaminase 2. *ACS Sens.* 10, 2760–2767. <https://doi.org/10.1021/acssensors.4c03460>.
- Hassert, R., Pagel, M., Ming, Z., Häupl, T., Abel, B., Braun, K., Wiessler, M., Beck-Sickinger, A.G., 2012. Biocompatible silicon surfaces through orthogonal click

- chemistries and a high affinity silicon oxide binding peptide. *Bioconjug. Chem.* 23, 2129–2137. <https://doi.org/10.1021/bc3003875>.
- Hatlem, D., Trunk, T., Linke, D., Leo, J.C., 2019. Catching a SPY: using the SpyCatcher-SpyTag and related systems for labeling and localizing bacterial proteins. *Int. J. Mol. Sci.* 20, 2129. <https://doi.org/10.3390/ijms20092129>.
- Heggestad, J.T., Fontes, C.M., Joh, D.Y., Hucknall, A.M., Chilkoti, A., 2020. Pursuit of zero 2.0: recent developments in nonfouling polymer brushes for immunoassays. *Adv. Mater.* 32, 1903285. <https://doi.org/10.1002/adma.201903285>.
- Hirsh, S.L., McKenzie, D.R., Nosworthy, N.J., Denman, J.A., Sezerman, O.U., Bilek, M.M.M., 2013. The vroman effect: competitive protein exchange with dynamic multilayer protein aggregates. *Colloids Surf. B Biointerfaces* 103, 395–404. <https://doi.org/10.1016/j.colsurfb.2012.10.039>.
- Hucknall, A., Rangarajan, S., Chilkoti, A., 2009. In pursuit of zero: polymer brushes that resist the adsorption of proteins. *Adv. Mater.* 21, 2441–2446. <https://doi.org/10.1002/adma.200900383>.
- Jiang, C., Wang, G., Hein, R., Liu, N., Luo, X., Davis, J.J., 2020. Antifouling strategies for selective in vitro and in vivo sensing. *Chem. Rev.* 120, 3852–3889. <https://doi.org/10.1021/acs.chemrev.9b00739>.
- Keeble, A.H., Banerjee, A., Ferla, M.P., Reddington, S.C., Anuar, I.N.A.K., Howarth, M., 2017. Evolving accelerated amidation by SpyTag/SpyCatcher to analyze membrane dynamics. *Angew. Chem. Int. Ed.* 56, 16521–16525. <https://doi.org/10.1002/anie.201707623>.
- Keeble, A.H., Turkki, P., Stokes, S., Khairil Anuar, I.N.A., Rahikainen, R., Hytönen, V.P., Howarth, M., 2019. Approaching infinite affinity through engineering of peptide–protein interaction. *Proc. Natl. Acad. Sci. U.S.A* 116, 26523–26533. <https://doi.org/10.1073/pnas.1909653116>.
- Keeble, A.H., Yadav, V.K., Ferla, M.P., Bauer, C.C., Chuntharpursat-Bon, E., Huang, J., Bon, R.S., Howarth, M., 2022. DogCatcher allows loop-friendly protein-protein ligation. *Cell Chem. Biol.* 29, 339–350.e10. <https://doi.org/10.1016/j.chembiol.2021.07.005>.
- Khairil Anuar, I.N.A., Banerjee, A., Keeble, A.H., Carella, A., Nikov, G.I., Howarth, M., 2019. Spy&Go purification of SpyTag-proteins using pseudo-SpyCatcher to access an oligomerization toolbox. *Nat. Commun.* 10, 1734. <https://doi.org/10.1038/s41467-019-09678-w>.
- Kimura, H., Miura, D., Tsugawa, W., Ikebukuro, K., Sode, K., Asano, R., 2021. Rapid and homogeneous electrochemical detection by fabricating a high affinity bispecific antibody–enzyme complex using two catcher/tag systems. *Biosens. Bioelectron.* 175, 112885. <https://doi.org/10.1016/j.bios.2020.112885>.
- Kinnamon, D.S., Heggestad, J.T., Liu, J., Chilkoti, A., 2022. Technologies for frugal and sensitive point-of-care immunoassays. *Annu. Rev. Anal. Chem.* 15, 123–149. <https://doi.org/10.1146/annurev-anchem-061020-123817>.
- Krishnan, N., Jiang, Y., Zhou, J., Mohapatra, A., Peng, F.-X., Duan, Y., Holay, M., Chekuri, S., Guo, Z., Gao, W., Fang, R.H., Zhang, L., 2024. A modular approach to enhancing cell membrane-coated nanoparticle functionality using genetic engineering. *Nat. Nanotechnol.* 19, 345–353. <https://doi.org/10.1038/s41565-023-01533-w>.
- Krishnan, N., Peng, F.-X., Mohapatra, A., Fang, R.H., Zhang, L., 2023. Genetically engineered cellular nanoparticles for biomedical applications. *Biomaterials* 296, 122065. <https://doi.org/10.1016/j.biomaterials.2023.122065>.
- Lebaudy, E., Guilbaud-Chéreau, C., Frisch, B., Vrana, N.E., Lavallo, P., 2023. The high potential of ε-Poly-L-Lysine for the development of antimicrobial biomaterials. *Adv. NanoBiomed. Res.* 3, 2300080. <https://doi.org/10.1002/anbr.202300080>.
- Lennicke, C., Cochemé, H.M., 2021. Redox metabolism: ROS as specific molecular regulators of cell signaling and function. *Mol. Cell* 81, 3691–3707. <https://doi.org/10.1016/j.molcel.2021.08.018>.
- Li, B., Jain, P., Ma, J., Smith, J.K., Yuan, Z., Hung, H.-C., He, Y., Lin, X., Wu, K., Pfandtner, J., Jiang, S., 2019. Trimethylamine N-oxide-derived zwitterionic polymers: a new class of ultralow fouling bioinspired materials. *Sci. Adv.* 5. <https://doi.org/10.1126/sciadv.aaw9562> eaaw9562.
- Ligorio, C., Mata, A., 2023. Synthetic extracellular matrices with function-encoding peptides. *Nat. Rev. Bioeng.* 1, 518–536. <https://doi.org/10.1038/s44222-023-00055-3>.
- Lowe, S., O'Brien-Simpson, N., Connal, L.A., 2015. Antibiofouling polymer interfaces: poly(ethylene glycol) and other promising candidates. *Polym. Chem.* 6, 198–212. <https://doi.org/10.1039/C4PY01356E>.
- Ma, H., Hyun, J., Stiller, P., Chilkoti, A., 2004. “Non-Fouling” oligo(ethylene glycol)-functionalized polymer brushes synthesized by surface-initiated atom transfer radical polymerization. *Adv. Mater.* 16, 338–341. <https://doi.org/10.1002/adma.200305830>.
- MacEwan, S.R., Chilkoti, A., 2010. Elastin-like polypeptides: biomedical applications of tunable biopolymers. *Peptide Sci.* 94, 60–77. <https://doi.org/10.1002/bip.21327>.
- Madl, C.M., Heilshorn, S.C., 2017. Tyrosine-selective functionalization for bio-orthogonal cross-linking of engineered protein hydrogels. *Bioconjug. Chem.* 28, 724–730. <https://doi.org/10.1021/acs.bioconjchem.6b00720>.
- Merckx, M., Smith, B., Jewett, M., 2019. Engineering sensor proteins. *ACS Sens.* 4, 3089–3091. <https://doi.org/10.1021/acssensors.9b02459>.
- Nowinski, A.K., Sun, F., White, A.D., Keefe, A.J., Jiang, S., 2012. Sequence, structure, and function of peptide self-assembled monolayers. *J. Am. Chem. Soc.* 134, 6000–6005. <https://doi.org/10.1021/ja3006868>.
- Pédelaq, J.-D., Cabantous, S., Tran, T., Terwilliger, T.C., Waldo, G.S., 2006. Engineering and characterization of a superfolder green fluorescent protein. *Nat. Biotechnol.* 24, 79–88. <https://doi.org/10.1038/nbt1172>.
- Postma, E.J., Scheres, L., de Beer, S., Kuzmyn, A.R., Zuilhof, H., 2025. Functionalized antifouling polymer brushes for biospecific surfaces. *Adv. Mater. Interfac.* 12, 2400955. <https://doi.org/10.1002/admi.202400955>.
- Qiang, X., Sun, K., Xing, L., Xu, Y., Wang, H., Zhou, Z., Zhang, J., Zhang, F., Caliskan, B., Wang, M., Qiu, Z., 2017. Discovery of a polystyrene binding peptide isolated from phage display library and its application in peptide immobilization. *Sci. Rep.* 7, 2673. <https://doi.org/10.1038/s41598-017-02891-x>.
- Riedel, T., Riedelová-Reichelová, Z., Májek, P., Rodriguez-Emmenegger, C., Houska, M., Dyr, J.E., Brynda, E., 2013. Complete identification of proteins responsible for human blood plasma fouling on poly(ethylene glycol)-based surfaces. *Langmuir* 29, 3388–3397. <https://doi.org/10.1021/la304886r>.
- Sauerbrey, G., 1959. Verwendung von Schwingquarzen zur Wägung dünner Schichten und zur Mikrowägung. *Z. Phys.* 155, 206–222. <https://doi.org/10.1007/BF01337937>.
- Song, X., Man, J., Qiu, Y., Wang, J., Liu, J., Li, R., Zhang, Y., Li, Jianyong, Li, Jianfeng, Chen, Y., 2024. Design, preparation, and characterization of lubricating polymer brushes for biomedical applications. *Acta Biomater.* 175, 76–105. <https://doi.org/10.1016/j.actbio.2023.12.024>.
- Stagge, F., Mitronova, G.Y., Belov, V.N., Wurm, C.A., Jakobs, S., 2013. Snap-, CLIP- and halo-tag labelling of budding yeast cells. *PLoS One* 8, e78745. <https://doi.org/10.1371/journal.pone.0078745>.
- Strader, R.L., Shmidov, Y., Chilkoti, A., 2024. Encoding structure in intrinsically disordered protein biomaterials. *Acc. Chem. Res.* 57, 302–311. <https://doi.org/10.1021/acs.accounts.3c00624>.
- Sun, F., Zhang, W.-B., Mahdavi, A., Arnold, F.H., Tirrell, D.A., 2014. Synthesis of bioactive protein hydrogels by genetically encoded SpyTag-SpyCatcher chemistry. *Proc. Natl. Acad. Sci.* 111, 11269–11274. <https://doi.org/10.1073/pnas.1401291111>.
- Sun, X.-B., Cao, J.-W., Wang, J.-K., Lin, H.-Z., Gao, D.-Y., Qian, G.-Y., Park, Y.-D., Chen, Z.-F., Wang, Q., 2019. SpyTag/SpyCatcher molecular cyclization confers protein stability and resilience to aggregation. *N. Biotech.* 49, 28–36. <https://doi.org/10.1016/j.nbt.2018.12.003>.
- Tang, Z., Palafox-Hernandez, J.P., Law, W.-C., Hughes, Z.E., Swihart, M.T., Prasad, P.N., Knecht, M.R., Walsh, T.R., 2013. Biomolecular recognition principles for bionanocombinatorics: an integrated approach to elucidate enthalpic and entropic factors. *ACS Nano* 7, 9632–9646. <https://doi.org/10.1021/nn404427y>.
- Tian, J., Liu, Y., Miao, S., Yang, Q., Hu, X., Han, Q., Xue, L., Yang, P., 2020. Amyloid-like protein aggregates combining antifouling with antibacterial activity. *Biomater. Sci.* 8, 6903–6911. <https://doi.org/10.1039/D0BM00760A>.
- Tyler, J., Ralston, C.Y., Rad, B., 2023. Sneaking in SpyCatcher using cell penetrating peptides for in vivo imaging. *Nanotechnology* 34, 425101. <https://doi.org/10.1088/1361-6528/acdf65>.
- Varanko, A.K., Su, J.C., Chilkoti, A., 2020. Elastin-like polypeptides for biomedical applications. *Annu. Rev. Biomed. Eng.* 22, 343–369. <https://doi.org/10.1146/annurev-bioeng-092419-061127>.
- Yang, W., Yang, D., Zhao, Z., Huang, C., Yan, B., Liu, Y., Zhang, L., Gong, L., Zeng, H., 2025. Hierarchically engineered triple-defensive antifouling coating with well-regulated structure for enhanced wastewater treatment. *Adv. Funct. Mater.* 35, 2420149. <https://doi.org/10.1002/adfm.202420149>.
- Zakeri, B., Fierer, J.O., Celik, E., Chittock, E.C., Schwarz-Linek, U., Moy, V.T., Howarth, M., 2012. Peptide tag forming a rapid covalent bond to a protein, through engineering a bacterial adhesin. *Proc. Natl. Acad. Sci.* 109, E690–E697. <https://doi.org/10.1073/pnas.1115485109>.
- Zhang, L., Vilà, N., Klein, T., Kohring, G.-W., Mazurenko, I., Walcarus, A., Etienne, M., 2016. Immobilization of cysteine-tagged proteins on electrode surfaces by thiol–ene click chemistry. *ACS Appl. Mater. Interfaces* 8, 17591–17598. <https://doi.org/10.1021/acsami.6b02364>.
- Zheng, C., Alvisi, N., de Haas, R.J., Zhang, Z., Zuilhof, H., de Vries, R., 2023. Modular design for proteins assembling into antifouling coatings: case of gold surfaces. *Langmuir*. <https://doi.org/10.1021/acs.langmuir.3c00389>.
- Zheng, C., Hussain, Z., Chen, C., de Haas, R.J., Deshpande, S., Zhang, Z., Zuilhof, H., de Vries, R., 2025a. One-step antifouling coating of polystyrene using engineered polypeptides. *J. Colloid Interface Sci.* 685, 350–360. <https://doi.org/10.1016/j.jcis.2025.01.147>.
- Zheng, C., Shmidov, Y., Varanko, A.K., Deshpande, S., Yang, Y., Shapiro, D.M., Zhang, Z., Zuilhof, H., Chilkoti, A., de Vries, R., 2025b. Nonfouling coatings from synthetic intrinsically disordered proteins. *Small*, 2504365. <https://doi.org/10.1002/smll.202504365>.